Korean Journal of Chemical Engineering
https://doi.org/10.1007/s11814-024-00225-y

ORIGINAL ARTICLE

Scalable Ammonia Synthesis in Fermentors Using Quantum Dot-*Azotobacter vinelandii* Hybrids

Jayeong Kim[1,2] · Byunghyun Lee[1,2] · Gui-Min Kim[1,2] · Ilsong Lee[1,2] · Sang Yup Lee[1,3,4] · Kyeong Rok Choi[1,3,5] · Doh C. Lee[1,2]

Received: 18 March 2024 / Revised: 7 June 2024 / Accepted: 9 July 2024

Abstract

This study introduces a scalable synthesis of ammonia through photochemical reactions, wherein nitrogen-fixing bacterial cells, *Azotobacter vinelandii* (*A. vinelandii*), form hybrids with colloidal quantum dots (QDs). Irradiation of the QD-*A. vinelandii* hybrids with visible light is found to significantly enhance ammonia production efficiency. The inherently low ammonia conversion rate of wild-type *A. vinelandii* is substantially increased upon incorporation of QDs. This increase is attributed to the electron transfer from QDs within the bacterial cells to intracellular bio-components. Transferring this chemistry to a large-scale reaction presents a tremendous challenge, as it requires precise control over the growth conditions. We explore the scalability of the QD-*A. vinelandii* hybrids by conducting the photochemical reaction in a 5-L fermentor under various parameters, such as dissolved oxygen, nutrient supply, and pH. Interestingly, ammonia was produced in media depleted of carbon sources. Consequently, a two-step fermentation process was designed, enabling effective ammonia production. Our findings demonstrate that the QD-*A. vinelandii* hybrid system in a bioreactor setup achieves an ammonia turnover frequency of 11.96 s^{-1}, marking a more than sixfold increase in efficiency over that of nitrogenase enzymes alone. This advancement highlights the potential of integrating biological and nanotechnological elements for scalable ammonia production processes.

Keywords Quantum Dot · Ammonia · Bacteria · *Azotobacter vinelandii* · Fermentation

Introduction

Ammonia is one of the most produced chemicals in the world, with its demand expanding significantly as both sources for fertilizers and hydrogen-storage media [1–4]. The increasing demand in these areas calls for sustainable synthesis of ammonia. The Haber–Bosch process, a conventional ammonia production process, is energy- and carbon-intensive in such a way that the process itself accounts for approximately 2% of global energy use and emits 2.9 tons of CO_2 for each ton of ammonia produced [5, 6]. Given these substantial energy demands and environmental ramification, there is a pressing need to explore new systems that offer improved energy efficiency and reduced environmental impact for ammonia synthesis.

The quest for sustainable ammonia production has led researchers to explore bio-based methods capitalizing on renewable resources. *Azotobacter vinelandii*, free-living nitrogen-fixing bacteria, convert atmospheric nitrogen into ammonia under ambient conditions. The nitrogenase

✉ Kyeong Rok Choi
choikr@kaist.ac.kr

✉ Doh C. Lee
dclee@kaist.edu

1 Department of Chemical and Biomolecular Engineering, Korea Advanced Institute of Science and Technology (KAIST), 291 Daehak-ro, Yuseong-gu, Daejeon 34141, Republic of Korea

2 Energy & Environmental Research Center (EERC), KAIST Institute for the Nanocentury (KINC), KAIST, Daejeon, Republic of Korea

3 Metabolic and Biomolecular Engineering National Research Laboratory, Systems Metabolic Engineering and Systems Healthcare Cross Generation Collaborative Laboratory, BioProcess Engineering Research Center, KAIST, Daejeon, Republic of Korea

4 BioInformatics Research Center, KAIST, Daejeon, Republic of Korea

5 R&D Center, GS Caltex Corporation, Yuseong-gu, Daejeon 34122, Republic of Korea

Published online: 13 August 2024

synthesizes ammonia through its enzymatic activity at temperatures below 40 °C and atmospheric pressure [7–12]. This biological process distinguishes itself from energy-intensive conventional methods by requiring significantly milder reaction conditions. However, the nitrogen fixation reaction orchestrated by these bacteria is inherently complex, resulting in a low ammonia production rate. The conversion of nitrogen to ammonia requires eight electrons and 16 adenosine triphosphate (ATP) molecules to synthesize two molecules of ammonia [10–14], and the hydrolysis of ATP is the rate-limiting step in the nitrogen fixation reaction [15, 16]. It is of paramount interest to facilitate the electron transfer in this step in order to increase the overall reaction rate of ammonia production from diazotrophs.

Colloidal quantum dots (QDs) are semiconductor nanocrystals in the quantum confinement regime. A set of unique optical and photophysical characteristics, such as size-tunable bandgap of semiconductors, has been the impetus for the precise control of their conduction and valence band energy levels. This property facilitates applications in high-resolution displays and LED lighting with enhanced brightness [17–19]. In addition, these properties open opportunities in catalysis and environmental applications, where their photoexcited electron–hole pair formation can catalyze chemical reactions [20–27]. In attempts to enhance ammonia synthesis, previous research demonstrated a hybrid system combining cadmium sulfide (CdS) nanorods with nitrogenase enzymes [28, 29]. This system achieved a notable turnover number of 1.1×10^4 mol NH_3 per mol of MoFe protein under constant light exposure for up to 5 h to catalyze chemical reactions effectively [28, 29]. However, previous approaches faced limitations due to the need for enzyme purification, the requirement for anaerobic conditions to maintain enzyme activity. In addition, the use of cadmium-based nanomaterials poses environmental and health risks. Addressing these challenges, our recent study has introduced a novel hybrid structure combining QDs with *A. vinelandii* [30]. This approach leverages a whole cell system to bypass preprocessing steps such as enzyme purification. The QD-*A. vinelandii* hybrid system, based on whole cells, not only overcomes the limitations associated with anaerobic activity but also utilizes the metabolic processes of living bacteria for real-time ammonia production under aerobic conditions. Furthermore, we utilized indium phosphide (InP)-based QDs, chosen for their biological compatibility due to being cadmium- and lead-free. We have developed a QD-*A. vinelandii* hybrid by integrating QDs into the bacterial growth process to facilitate their internalization. This system is capable of efficient photoinduced ammonia production, marking a significant step forward in sustainable ammonia-synthesis technology.

Producing materials from renewable biomass in biorefineries has become increasingly important for global sustainability goals. This study advances this effort by demonstrating the scalable cultivation of *A. vinelandii* in fermentors [21, 31, 32]. We facilitated bench-scale cultivation of nitrogen-fixing bacteria using a fermentor to examine the system's scalability. Fermentation plays a crucial role in sustainable chemical production, offering solutions to global environmental challenges [7, 33, 34]. The implementation of QD-*A. vinelandii* hybrid structures in the fermentation process holds great significance.

The effective cultivation of inoculated bacterial seed culture to high concentration of cells is essential. To address these challenges, dissolved oxygen (DO) levels and nutrient concentrations in the culture medium were regulated for successful high-density cultivation. Upon reaching maximum bacterial density, light irradiation was applied to activate the QD-*A. vinelandii* hybrids for ammonia synthesis. This research aims to develop a method for producing ammonia that is both efficient and environmentally sustainable, providing a milder alternative to the existing Haber–Bosch process by using the hybrid of nitrogen-fixing bacteria and QDs.

Experimental

Materials

Indium acetate ($In(OAc)_3$, 99.99%), Zinc acetate ($Zn(OAc)_2$, 99.99%), oleic acid (OA, 90%), 1-octadecene (ODE, 98%), tri-*n*-octylphosphine (TOP, 97%), tris(trimethylsilyl)phosphine ($P(SiMe_3)_3$, ≥ 95%), tetramethylammonium hydroxide pentahydrate ($TMAH \cdot 5H_2O$, ≥ 97%), 3-mercaptopropionic acid (MPA, ≥ 99%), iron (III) chloride ($FeCl_3$, anhydrous powder, ≥ 99.99%), sodium molybdate dihydrate ($Na_2MoO_4 \cdot 2H_2O$, ≥ 99.5%), sodium citrate monobasic (anhydrous, ≥ 99.5%), salicylic acid (≥ 99%), sodium hypochlorite solution (NaClO, 10–15% chlorine), sodium nitroferricyanide(III) dihydrate ($Na_2[Fe(CN)_5NO] \cdot 2H_2O$, ≥ 98%) and Dulbecco's Phosphate Buffered Saline (D8537, PBS) were purchased from Sigma-Aldrich. Saccharose (sucrose, EP, GR) and sodium hydroxide (NaOH, 97%) were purchased from JUNSEI. Burk's medium (sucrose (20 g/L), $MgSO_4$ (0.2 g/L), K_2HPO_4 (0.8 g/L), KH_2PO_4 (0.2 g/L), $CaSO_4$ (0.13 g/L), $FeCl_3$ (1.45 mg/L), and Na_2MoO_4 (0.253 mg/L)) was purchased from HIMEDIA. All the purchased chemicals were used without further purification. *A. vinelandii* (KCTC 2426, ATCC 12837) was obtained from the Korean Collection for Type Cultures.

Colloidal InP/ZnSe Core–Shell Quantum Dots

InP QDs were synthesized via the heat-up method following established procedures [30, 35, 36]. In a 100-mL three-neck round-bottom flask, 0.45 mmol of $In(OAc)_3$, 1.35 mmol of OA, and 27 mL of ODE were combined. After degassing at 120 °C, 2.2 mL of TOP was introduced under argon atmosphere. Following 30 min of degassing, the mixture was cooled to room temperature in an argon atmosphere. A solution of 0.3 mmol of $P(SiMe3)_3$ in 0.9 mL of TOP was injected into the reactor at room temperature, and the temperature was raised to 300 °C. The InP core was annealed for 5 min at 300 °C and then cooled to room temperature. For the ZnSe shell, the successive ionic layer adsorption and reaction (SILAR) method was employed. A zinc precursor, consisting of 10 mmol of $Zn(OAc)_2$, 20 mmol of OA, and 13.7 mL of ODE, was degassed at 120 °C. After the addition of 5 mL of TOP, further degassing occurred for 30 min. The flask was heated to 250 °C to form Zinc oleate ($Zn(OA)_2$) for 30 min and cooled to 120 °C. This process was repeated for cooling to 60 °C. The $Zn(OA)_2$ was then injected into the InP core QDs, while 2 M of TOP-Se was added dripwise as the anion precursors, with the amount calculated based on the relation between the volume of the ZnSe monolayer and the number of core dots. The synthesized QDs were initially dispersed in toluene and underwent purification with ethanol, isopropanol, and butanol as anti-solvents. The QDs were subjected to centrifugation and then redispersed in toluene, repeating this purification process three times. Subsequently, the purified QDs in toluene were mixed with an MPA solution (0.2 M MPA, 0.35 M TMAH $5H_2O$ in methanol) and sonicated for 30 min. In the ligand-exchange process, hexane and acetone served as anti-solvents, and the precipitation process was repeated three times. Finally, the MPA-capped InP/ZnSe QDs were dissolved in deionized water. The synthesized QDs were imaged using field-emission transmission electron microscopy (TEM) (Tecnai F20, FEI Company). Absorption spectra of QDs were recorded using a UV–Vis spectrometer (UV3600, Shimadzu). Emission spectra were obtained with a photoluminescence spectrometer (C11347, Hamamatsu).

Quantum Dot-*A. vinelandii* Hybrid

A. vinelandii was cultured in a modified Burk's medium containing adjusted concentrations of $FeCl_3$ and Na_2MoO_4 to 8 and 2.45 mg/L, respectively [23]. The bacterial seed culture were transferred to a fresh Burk's medium in a 250 mL flask with a 1/100 dilution after 30 h of cultivation at 30 °C with rotary shaking at 200 rpm. The QD-*A. vinelandii* hybrid cells were prepared by co-cultivating bacteria and QDs simultaneously in a culture medium. For making the QD-*A. vinelandii* hybrid cells, the pre-cultured bacteria were inoculated into the modified Burk's medium including sterile-filtered QDs and were cultivated at 30 °C with rotary shaking at 200 rpm in a 250-mL flask. QDs were sterilized by filtration through a hydrophilic 0.2-μm pore syringe filter. The concentration of QDs in the culture medium was set to 50 nM (Fig. S1). The grown cells were washed with cold PBS three times. The optical density at 600 nm (OD_{600}) for confirming cell density was adjusted to 2.0 using a TECAN Infinite 200PRO (200 μL of sample per well of a 96-well plate, without dilution for measurement), and then 2 mL of the cell suspension was exposed to light (Supplementary Note 1). In the flask-scale experiments, we used OSRAM DULUX L 36W/864 lamps (6500 K, 53 mW) as white light sources. For the fermentation experiments, LED panels were used, and the spectrum data are shown in Fig. S2. This section describes the conditions specific to the flask-scale experiments.

Determination of Dry Cell Weight

To measure the dry cell weight (DCW), a 10 mL of cell suspension of *A. vinelandii* adjusted to an OD_{600} of 2.0 (measured using TECAN Infinite 200PRO without dilution; 200 μL of sample per well of 96-well plate) was centrifuged at 8000 rpm for 5 min. The resulting cell pellet was then collected, dried, and weighed. This method determined that the DCW of our samples at OD_{600} 2.0 was 8.43 g/L.

Quantification of Ammonia

To quantify ammonia concentrations in cell culture supernatants, the indophenol blue colorimetric method was employed [30, 37]. Cell culture supernatants were obtained by diluting cell cultures in PBS, and the supernatant was collected for analysis. Standard ammonium-ion solutions with known concentrations were prepared for the calibration curve and the calibration curve was drawn for each quantification to enhance the reliability. Indophenol blue reagents were added sequentially to each standard solution and supernatant of samples. The reaction was allowed to proceed for 2 h at room temperature and the absorbance measurements were conducted at 655 nm using a spectrophotometer.

Fermentation

In this study, *A. vinelandii* was cultivated in a fermentor, which is a bioreactor. Unlike microbial cultivation at the flask scale, certain factors are essential to optimize bacterial growth in fermentor. The prepared *A. vinelandii* in 200 mL of modified Burk's medium as seed culture was inoculated into the 1.8 L of modified Burk's medium containing sterile-filtered QDs. The pH was maintained at

7.50 using 1 M NaOH. To ensure optimal conditions, the fermentation process was carried out at a temperature of 30 °C. The DO level was controlled in the range of 10–40% through the regulation of air flow rate and agitation. Throughout the fermentation, cell density was monitored using UV–Vis spectroscopy, measuring the optical density at a wavelength of 600 nm. The bacterial fermentation was performed using Liflux GX equipment by Hanil Science. The concentration of sucrose was measured by HPLC (1515 isocratic HPLC pump, Waters) equipped with a refractive index detector (2414, Waters) and MetaCarb 87H column (Agilent). Samples were filtered using a 0.22-µm pore PVDF (polyvinylidene fluoride) syringe filter and were eluted isocratically with 0.005 M H_2SO_4 at 35 °C at a flow rate of 0.5 mL/min. This section details the conditions specific to the fermentor scale experiments.

Results and Discussion

Colloidal Quantum Dots as Photosensitizers

We introduce a system for producing ammonia by integrating QDs within bacteria and applying light irradiation to the QD-*A. vinelandii* hybrids, as shown in Fig. 1a. Harnessing QDs as photosensitizers in photochemical reactions requires the design and synthesis of QDs with facile charge extraction capabilities. In this research, core–shell structured QDs were engineered with water-dispersible ligands for efficient interaction in a whole cell system. InP core QDs were uniformly synthesized using the heat-up method. The synthesis of ZnSe shells via SILAR method resulted in a quasi-type II bandgap structure in the core–shell QDs [30, 35, 36, 38]. Furthermore, the oleic acid ligands on the surface of the QDs were replaced with mercaptopropionic acid to improve their dispersion and reactivity of QDs in aqueous solutions. The absorption and photoluminescence spectra of the InP/ZnSe core–shell QDs, as depicted in Fig. 1b, explain the optical properties of QDs. Notably, the 1S peak wavelength of the InP core, detailed in Fig. S3, is observed at 460 nm, indicating a bandgap energy of approximately 2.70 eV for the core QDs. An increase in shell thickness leads to a decrease in the quantum confinement effect and lowers the energy level at the conduction band edge. This increase in shell synthesis leads to the formation of the quasi-type II bandgap alignment, a critical feature designed to improve electron extraction capabilities significantly [39]. The generated holes are scavenged by glutathione (GSH) molecules, which are oxidized to glutathione disulfide (GSSG) [40]. Figure S4 shows a significant decrease in GSH concentration, as indicated by the reduced absorbance at 412 nm. This confirms that GSH effectively scavenges the holes generated during electron transfer in QDs, thereby stabilizing the system and enhancing the photochemical activity of the QDs. The characterization of these QDs reveals their distinct sizes as visually confirmed by the TEM image in Fig. 1c.

Influence of Light Sources on Cell Viability

Ammonia production efficiency under a 400 nm light source reached saturation after 6 h. This outcome indicates limited ammonia productivity under 400 nm light, hypothesized to result from cellular damage. 400 nm light sources, known to generate reactive oxygen species (ROS) within cells, potentially compromise cellular viability [41–43]. To address these challenges and enhance the overall efficiency of the hybrid system, experiments utilized white light, chosen for

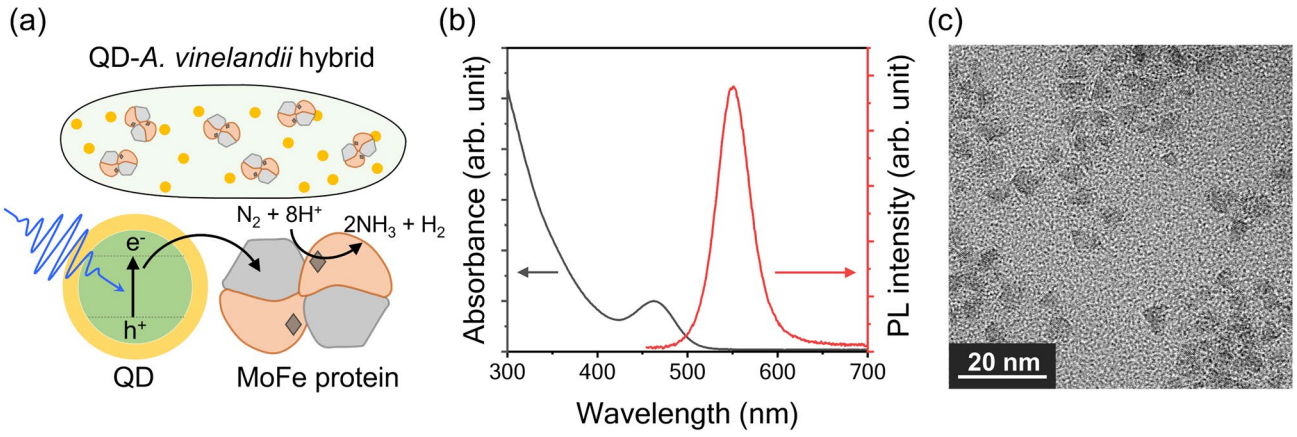

Fig. 1 **a** Schematic illustration of QD-*A. vinelandii* hybrid for ammonia synthesis, highlighting the interaction between QDs and bacterial cells. **b** Absorption and photoluminescence spectra of InP/ZnSe QDs, demonstrating their optical characteristics. **c** Transmission electron microscopy (TEM) image of InP/ZnSe QDs

its high light-absorption capabilities of QDs and optimized wavelength to minimize cellular damage.

Ammonia production under white light irradiation continued to increase and this demonstrated an extended productive phase compared to 400 nm light conditions (Fig. 2a). Unlike the results obtained with 400 nm light exposure where ammonia production reached saturation at 6 h, the QD-*A. vinelandii* hybrid cells exposed to white light demonstrate a continuous increase in ammonia production for up to 12 h. In Fig. 2b, the number of viable cells over time during the ammonia production reaction is shown, with data comparing the effects of various light sources on cell density. Notably, a significant decline in cell viability under 400 nm light was observed around the 4-h mark, in contrast to cells maintained in dark. In comparison, bacteria exposed to white light resulted in a substantially higher survival rate than the case of 400 nm light irradiation. This condition effectively delayed the saturation of ammonia production.

Nitroblue tetrazolium (NBT) was employed to compare the amount of ROS generated. The NBT assay allows for the comparison of ROS levels by observing changes in absorbance at 560 nm, which result from the formation of the reduced form of NBT, known as NBT formazan [44, 45]. Upon excitation with monochromatic light of 400 nm wavelength, QDs generate more ROS than those under dark or white light conditions (Fig. 2c and Fig. S5). This result supports the previous assumption that the elevated levels of ROS production under 400 nm light could inflict damage on the cells.

Furthermore, the observations suggest that ROS may not be the sole factor contributing to cellular damage in our QD-*A. vinelandii* hybrid system. First, the GSH depletion is significant. GSH is integral for maintaining redox balance and defending bacterial cells against various toxic compounds and stressors [40]. In our hybrid system, exposure to light induces oxidation of GSH, leading to a notable reduction in intracellular GSH levels, as evidenced by our findings in Fig. S4. This depletion of available GSH, which is critical for defending against oxidative stress, likely contributes to increased cellular damage, subsequently reducing viable cell density. Second, changes in the availability of metabolic cofactors such as NAD(P)H, which serve as electron shuttles, could also impact cellular metabolism. Change in the cofactor levels could alter the metabolic activity, which could potentially decrease cell density. These mechanisms together provide a broader explanation for the observed decrease in cell viability, indicating a complex interplay of factors.

Moreover, an investigation was conducted on the ammonia synthesis by bacteria under illumination in the absence of QDs, to ascertain that the observed enhancement in production stemmed from photoexcited charges elicited by the QDs, rather than from mere light exposure (Fig. S6). The experiments resulted in no increase in ammonia production when only light was applied, indicating that the enhancement in ammonia production is directly or indirectly attributed to the photoexcited charges generated by the QDs.

Effect of Growth Medium and Nutrients on Ammonia Production

In ongoing experimental investigations, the ammonia-synthesis system of dispersed hybrid cells in phosphate-buffered saline (PBS) was conducted after removing the nutrient media. Ammonia production was not observed under conditions of nutrient-rich media. This observation leads to the hypothesis that bacteria, when provided with ample nutrients, preferentially engage in metabolic activities

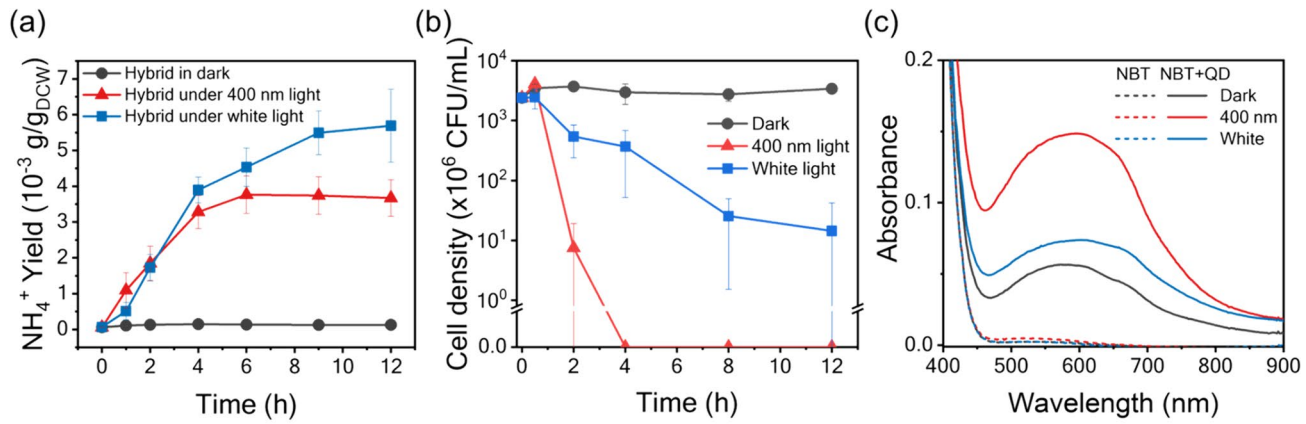

Fig. 2 **a** Ammonia production and **b** viable cell density changes of QD-*A. vinelandii* hybrids over time, both under two distinct light wavelengths, 400 nm and white light, with a consistent light intensity of 8 mW for each condition. Ammonia yield is calculated by dividing the ammonia concentration by the dry cell weight (DCW) of *A. vinelandii*. **c** Comparative analysis of reactive oxygen species (ROS) levels utilizing the nitroblue tetrazolium (NBT) assay to measure the effects of various light conditions

related to biomass formation. The research focused on assessing the roles of sucrose and magnesium ion (Mg^{2+}) in the ammonia production efficiency of QD-*A. vinelandii* hybrids. Sucrose serves as the primary carbon source for cellular growth and energy production. Mg^{2+} is essential for enzyme activation, maintaining cellular and genetic integrity, and efficient nitrogen fixation [46].

Adding carbon resources to the PBS buffer inhibited ammonia production. This suggests that providing carbon is insufficient to stimulate ammonia synthesis in the hybrid cells (Fig. 3a). Conversely, Fig. 3b shows that removing sucrose from Burk's medium resulted in increased ammonia productivity. This indicates that sucrose supply can influence metabolic shifts within the cells. Under conditions rich in nutrients, bacteria appear to prioritize biomass formation (Fig. S7). This process leads to the continuous utilization and subsequent depletion of any ammonia produced, making it nearly undetectable. In contrast, under PBS conditions with limited essential carbon sources, bacteria shift their metabolic focus, preventing biomass formation and enabling ammonium-ion accumulation. The absence of sucrose might mitigate a competitive metabolic pathway, thereby enhancing the efficiency of ammonia synthesis. These observations highlight the importance of a delicate balance between nutrient availability and metabolic activity for the optimization of the QD-*A. vinelandii* hybrid system for ammonia production. Further experimentation involved subjecting a series of hybrid cell cultures to a single feeding of sucrose at different reaction times for up to 12 h. The results shown in Fig. S8 revealed that cells supplemented with sucrose early in the reaction period produced the least ammonia. Conversely, samples fed sucrose at later stages, particularly at 9 h, demonstrated increased ammonia production, closely rivaling that of cultures without any sucrose feeding. This emphasizes the importance of balanced nutrient management in optimizing the QD-*A. vinelandii* hybrid system for efficient ammonia synthesis.

Further analysis on the effect of Mg^{2+} supplementation or its removal showed that ammonia productivity remained consistent. This suggests that Mg^{2+} does not significantly influence ammonia production in the QD-*A. vinelandii* hybrid system. As shown in Fig. 3c, this observation highlights the pivotal contribution of QDs, possibly via photoinduced charge transfers, in the ammonia-synthesis process, surpassing traditional nutrient factors such as Mg^{2+}. The minimal impact of Mg^{2+} on ammonia production indirectly validates the critical contribution of QDs to the system. Their important roles in enhancing ammonia-synthesis efficiency are paramount.

A. vinelandii primarily utilizes magnesium salt of ATP (MgATP) for activation of nitrogenase in nitrogen fixation metabolism [47]. The presence of magnesium ions is essential for efficient ATP hydrolysis, which facilitates electron transfer within the cell. In the absence of magnesium, the rate of ATP hydrolysis decreases, potentially reducing the ammonia production capability of the bacteria.

One-Pot Synthesis of Ammonia Using QD-*A. vinelandii* Hybrid

Despite sucrose's ability to promote bacterial proliferation, our insights reveal that removing sucrose establishes optimal conditions for enhanced ammonia synthesis. Building on these insights, we proposed a separated process comprising a cultivation step conducted in dark conditions—allowing QD-*A. vinelandii* to sufficiently internalize and grow while depleting sucrose in the culture medium—and a subsequent production step induced by light exposure to generate

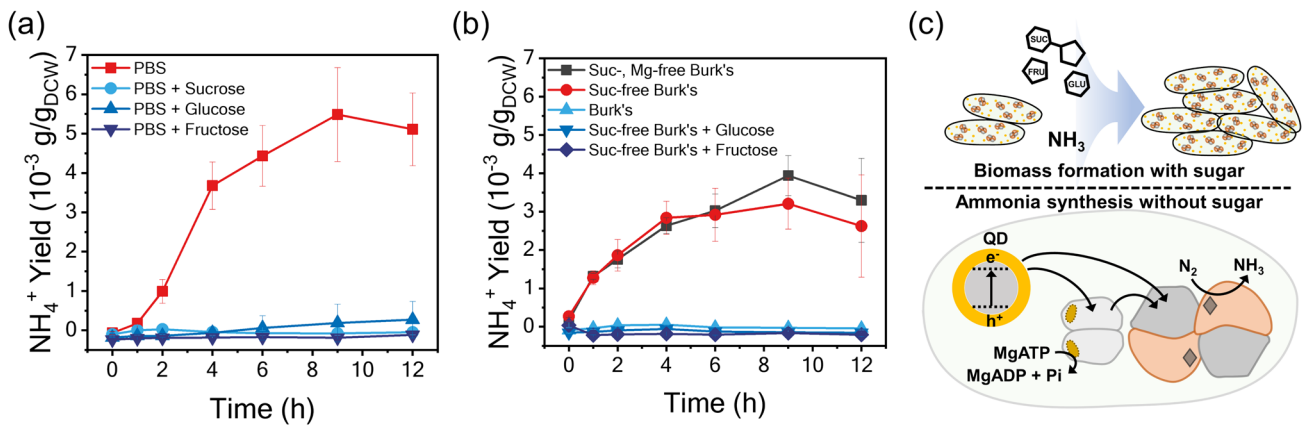

Fig. 3 **a** Ammonia production in PBS supplemented with sugars, and **b** ammonia production in sucrose or magnesium free Burk's medium, including the addition of different sugars. These experiments collectively elucidate the effects of light, nutrient composition, and environmental conditions on the ammonia production capabilities of QD-*A. vinelandii* hybrids. **c** Schematic illustration of the effect of sucrose or magnesium on ammonia synthesis in QD-*A. vinelandii* hybrids

ammonia. The overview of this two-step process is depicted in Fig. 4a.

Furthermore, appropriate DO levels were crucial for the fermentation of *A. vinelandii*, an aerobic bacterium with enzymes that are active under anaerobic conditions. The anaerobic bacteria require a balanced air supply for optimal growth and ammonia production. In experiments comparing bacterial growth across DO levels from 10 to 40%, we observed that a controlled DO level at 10% (Fig. 4b) facilitated the conditions needed for both biomass formation and efficient ammonia synthesis. This adjustment in oxygen levels reflects a strategic approach to optimizing the conditions for ammonia production without compromising bacterial growth.

In the conducted fermentation experiments, an elevated level of ammonia production was observed through the QD-*A. vinelandii* hybrid system, as shown in Fig. 4c. *A. vinelandii* cultured in a nutrient medium containing QDs and sucrose under dark conditions, exhibited growth with an OD_{600} value of approximately 23, which corresponds to 3.71 g/L of dry cell weight (DCW). Subsequently, the sucrose in the culture medium was completely depleted and light irradiation was started to stimulate ammonia production. The amount of ammonia produced reached approximately 7.8 mg/L for a 45-h reaction period, significantly surpassing the turnover frequency (TOF) of enzymes responsible for ammonia generation within conventional nitrogenase in nitrogen-fixing bacteria. The TOF, calculated by dividing the moles of synthesized ammonia per time by the moles of MoFe protein, showed our hybrid system's TOF value to be an impressive 11.96 s^{-1}, with the moles of MoFe protein per DCW approximated to 9.02×10^{-11} (Fig. 4d and Supplementary Note 2). This demonstrates a remarkable difference in ammonia productivity by over sixfold compared to conditions using purified MoFe proteins with the presence of Fe proteins and ATPs [21]. Specifically, the fermentation of the QD-*A. vinelandii* hybrid system resulted in ammonia production with a titer of 7.81 mg/L, a yield of 7.41 mmol/mol, and a productivity of 0.174 mg/L/h. Our approach has led to significant advancements and efficiency in ammonia synthesis. It highlights the potential of the QD-*A. vinelandii* hybrid system for enhancing bioengineering applications.

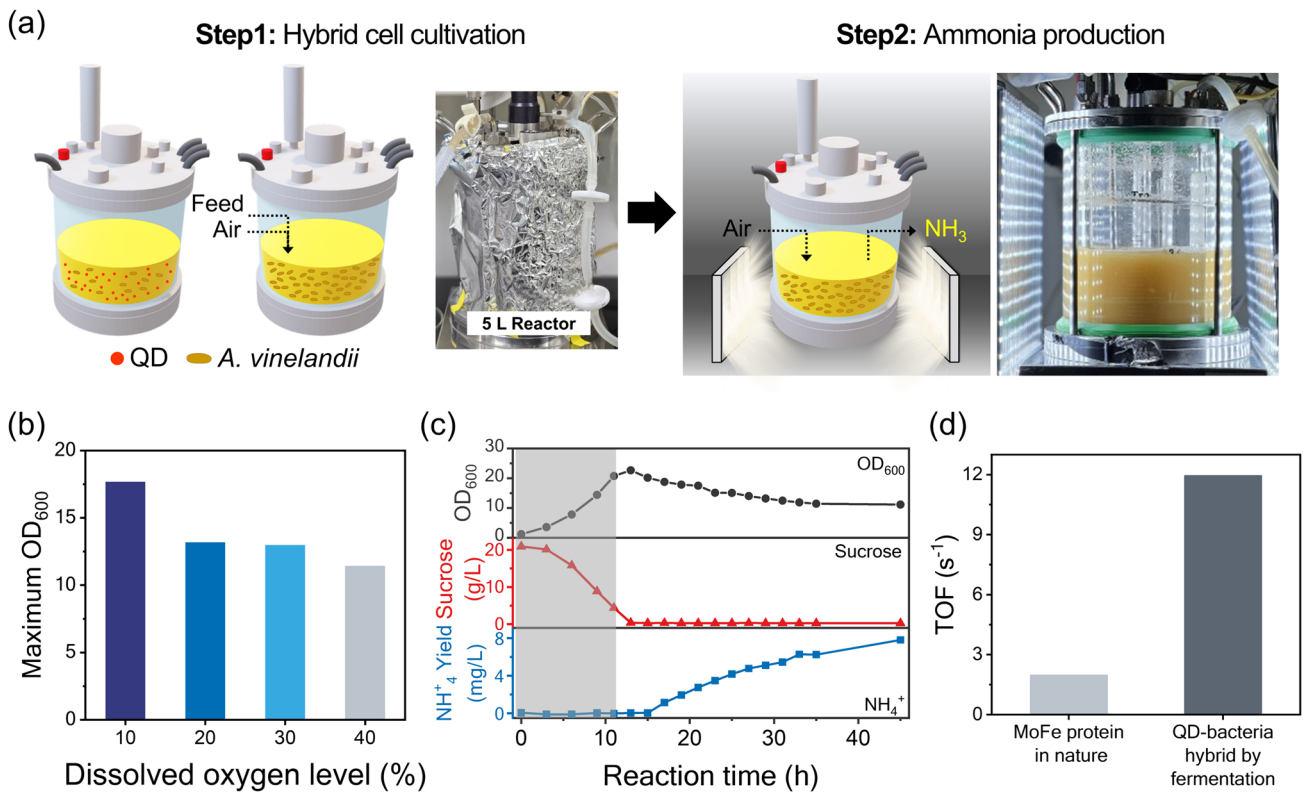

Fig. 4 **a** Overview of the one-pot fermentation process for ammonia synthesis. **b** Comparing maximum cell densities under varying dissolved oxygen (DO) levels in fermentation process. The saturated DO value of the bacteria-free nutrient medium is set to 100%. **c** Bacterial growth, sucrose consumption, and ammonia production of the QD-*A. vinelandii* hybrid through fermentation by reaction time. **d** Comparison of turnover frequency (TOF) between the MoFe protein and the QD-*A. vinelandii* hybrid system in the fermentation process for ammonia synthesis

Conclusion

This study presents a scalable approach to ammonia production using hybrid of QDs and nitrogen-fixing bacteria in fermentors. Our comprehensive investigation of the QD-*A. vinelandii* hybrid system yielded valuable insights into optimizing the fermentation conditions of *A. vinelandii*. The research progressed from laboratory scale experiments to bench scale studies, representing a significant advancement toward the practical implementation of this system.

The uptake of core–shell structured QDs into *A. vinelandii* enhances charge dissociation probability, which is pivotal for efficient photochemical reactions. The transition to white light as a source minimized phototoxic effects on the bacteria, and effectively prolonged ammonia production beyond the constraints of conventional 400 nm irradiation. In addition, while the presence of sucrose led to ammonia consumption for biomass formation, its depletion significantly increased ammonia productivity. To address this, a two-step fermentation process was developed, first involving a dark cultivation phase followed by a light-exposed production phase, which not only facilitates bacterial growth but also enhances ammonia productivity, effectively overcoming the difficulties encountered due to restricted ammonia production in standard growth media with sucrose. Furthermore, our comparison of ammonia production efficiency with Mg^{2+} content indirectly confirmed the role of QDs in enhancing ammonia synthesis.

These findings significantly advance QD-*A. vinelandii* hybrid applications in sustainable ammonia synthesis. The integration of nanomaterials and biological systems holds great promise for environmentally benign technologies.

Supplementary Information The online version contains supplementary material available at https://doi.org/10.1007/s11814-024-00225-y.

Acknowledgements This work has been supported by the Samsung Research Funding & Incubation Center of Samsung Electronics under Project Number SRFC-MA2001-07, the National Research Foundation of Korea (NRF) under Project Number 2022R1A5A1033719 and 2022M3J5A1056117, and the Korea Planning & Evaluation Institute of Industrial Technology (KEIT) under Project Number 20019417.

Funding Open Access funding enabled and organized by KAIST. Samsung Research Funding; Incubation Center of Samsung Electronics, SRFC-MA2001-07, Doh Chang Lee, National Research Foundation of Korea (NRF), 2022R1A5A1033719, Doh Chang Lee, 2022M3J5A1056117, Sang Yup Lee,Korea Planning; Evaluation Institute of Industrial Technology (KEIT), 20019417, Doh Chang Lee.

References

1. K.H. Rouwenhorst, G. Castellanos. Innovation outlook: renewable ammonia (Irena, 2022)
2. S. Giddey, S. Badwal, C. Munnings, M. Dolan, ACS Sustain. Chem. Eng. **5**, 10231–10239 (2017)
3. S. Wu, N. Salmon, M.M.-J. Li, R. Bañares-Alcántara, S.C.E. Tsang, ACS Energy Lett. **7**, 1021–1033 (2022)
4. D.R. MacFarlane, P.V. Cherepanov, J. Choi, B.H. Suryanto, R.Y. Hodgetts, J.M. Bakker, F.M.F. Vallana, A.N. Simonov, Joule **4**, 1186–1205 (2020)
5. C. Smith, A.K. Hill, L. Torrente-Murciano, Energy Environ. Sci. **13**, 331–344 (2020)
6. J.W. Erisman, M.A. Sutton, J. Galloway, Z. Klimont, W. Winiwarter, Nat. Geosci. **1**, 636–639 (2008)
7. M.H. Plunkett, C.M. Knutson, B.M. Barney, Microb. Cell Fact. **19**, 1–12 (2020)
8. Y. Hu, M.W. Ribbe, Biochim. Biophys. Acta (BBA)-Bioenerg. **1827**, 1112–1122 (2013)
9. K. Tanifuji, Y. Ohki, Chem. Rev. **120**, 5194–5251 (2020)
10. B.M. Hoffman, D. Lukoyanov, Z.-Y. Yang, D.R. Dean, L.C. Seefeldt, Chem. Rev. **114**, 4041–4062 (2014)
11. J. Kästner, S. Hemmen, P.E. Blöchl, J. Chem. Phys. **123**, 074306 (2005)
12. J. Kästner, P.E. Blöchl, J. Am. Chem. Soc. **129**, 2998–3006 (2007)
13. K. Danyal, S. Shaw, T.R. Page, S. Duval, M. Horitani, A.R. Marts, D. Lukoyanov, D.R. Dean, S. Raugei, B.M. Hoffman, Proc. Natl. Acad. Sci. **113**, E5783–E5791 (2016)
14. S.L. Foster, S.I.P. Bakovic, R.D. Duda, S. Maheshwari, R.D. Milton, S.D. Minteer, M.J. Janik, J.N. Renner, L.F. Greenlee, Nat. Catal. **1**, 490–500 (2018)
15. Z.-Y. Yang, R. Ledbetter, S. Shaw, N. Pence, M. Tokmina-Lukaszewska, B. Eilers, Q. Guo, N. Pokhrel, V.L. Cash, D.R. Dean, Biochem. **55**, 3625–3635 (2016)
16. S. Duval, K. Danyal, S. Shaw, A.K. Lytle, D.R. Dean, B.M. Hoffman, E. Antony, L.C. Seefeldt, Proc. Natl. Acad. Sci. **110**, 16414–16419 (2013)
17. D.-E. Yoon, S. Yeo, H. Lee, H. Cho, N. Wang, G.-M. Kim, W.K. Bae, Y.K. Lee, Y.-S. Park, D.C. Lee, Chem. Mater. **34**, 9190–9199 (2022)
18. N. Wang, S. Koh, B.G. Jeong, D. Lee, W.D. Kim, K. Park, M.K. Nam, K. Lee, Y. Kim, B.-H. Lee, Nanotechnology **28**, 185603 (2017)
19. D.J. Shin, H. Jang, D. Kim, J.Y. Woo, Y.K. Lee, W.K. Bae, J. Kim, Y.-S. Park, D.C. Lee, Appl. Surf. Sci. **614**, 156160 (2023)
20. J.R. Bertram, Y. Ding, P. Nagpal, Nanoscale Adv. **2**, 2363–2370 (2020)
21. Y. Ding, J.R. Bertram, C. Eckert, R.R. Bommareddy, R. Patel, A. Conradie, S. Bryan, P. Nagpal, J. Am. Chem. Soc. **141**, 10272–10282 (2019)
22. S. Cestellos-Blanco, J.M. Kim, N.G. Watanabe, R.R. Chan, P. Yang, Iscience **24**, 102952 (2021)

23. N. Kornienko, K.K. Sakimoto, D.M. Herlihy, S.C. Nguyen, A.P. Alivisatos, C.B. Harris, A. Schwartzberg, P. Yang, Proc. Natl. Acad. Sci. **113**, 11750–11755 (2016)
24. N. Wang, S. Cheong, D.-E. Yoon, P. Lu, H. Lee, Y.K. Lee, Y.-S. Park, D.C. Lee, J. Am. Chem. Soc. **144**, 16974–16983 (2022)
25. D. Lee, W.D. Kim, S. Lee, W.K. Bae, S. Lee, D.C. Lee, Chem. Mater. **27**, 5295–5304 (2015)
26. H. Cho, W. Dongim, J. Yu, S. Lee, D.C. Lee, ChemCatChem **10**, 5679–5688 (2018)
27. W.D. Kim, J.-H. Kim, S. Lee, S. Lee, J.Y. Woo, K. Lee, W.-S. Chae, S. Jeong, W.K. Bae, J.M. Seok, D.C. Lee, Chem. Mater. **28**, 962–968 (2016)
28. K.A. Brown, D.F. Harris, M.B. Wilker, A. Rasmussen, N. Khadka, H. Hamby, S. Keable, G. Dukovic, J.W. Peters, L.C. Seefeldt, Science **352**, 448–450 (2016)
29. L.M. Pellows, M.A. Willis, J.L. Ruzicka, B.P. Jagilinki, D.W. Mulder, Z.-Y. Yang, L.C. Seefeldt, P.W. King, G. Dukovic, J.W. Peters, Nano Lett. **23**, 10466–10472 (2023)
30. S. Koh, Y. Choi, I. Lee, G.-M. Kim, J. Kim, Y.-S. Park, S.Y. Lee, D.C. Lee, J. Am. Chem. Soc. **144**, 10798–10808 (2022)
31. H. Zhang, H. Liu, Z. Tian, D. Lu, Y. Yu, S. Cestellos-Blanco, K.K. Sakimoto, P. Yang, Nat. Nanotechnol. **13**, 900–905 (2018)
32. Q. Hu, H. Hu, L. Cui, Z. Li, D. Svedruzic, J.L. Blackburn, M.C. Beard, J. Ni, W. Xiong, X. Gao, ACS Energy Lett. **8**, 677–684 (2022)
33. J.H. Ahn, H. Seo, W. Park, J. Seok, J.A. Lee, W.J. Kim, G.B. Kim, K.-J. Kim, S.Y. Lee, Nat. Commun. **11**, 1970 (2020)
34. K.R. Choi, S.Y. Lee, Nat. Rev. Bioeng. **1**, 832–857 (2023)
35. P. Ramasamy, N. Kim, Y.-S. Kang, O. Ramirez, J.-S. Lee, Chem. Mater. **29**, 6893–6899 (2017)
36. Z. Xu, Y. Li, J. Li, C. Pu, J. Zhou, L. Lv, X. Peng, Chem. Mater. **31**, 5331–5341 (2019)
37. G.-E. Park, H.-N. Oh, S.-Y. Ahn, Bull. Korean Chem. Soc. **30**, 2032–2038 (2009)
38. S.-H. Wei, A. Zunger, Appl. Phys. Lett. **72**, 2011–2013 (1998)
39. C. Pak, J.Y. Woo, K. Lee, W.D. Kim, Y. Yoo, D.C. Lee, J. Phys. Chem. C **116**, 25407–25414 (2012)
40. G. Smirnova, N. Muzyka, O. Oktyabrsky, Microbiol. Res. **167**, 166–172 (2012)
41. L. Wang, C. Hu, L. Shao, Int. J. Nanomedicine **12**, 1227–1249 (2017)
42. W. He, H.-K. Kim, W.G. Wamer, D. Melka, J.H. Callahan, J.-J. Yin, J. Am. Chem. Soc. **136**, 750–757 (2014)
43. I. Lee, J. Moon, H. Lee, S. Koh, G.-M. Kim, L. Gauthé, F. Stellacci, Y.S. Huh, P. Kim, D.C. Lee, Biomater. Sci. **10**, 7149–7161 (2022)
44. H.S. Choi, J.W. Kim, Y.N. Cha, C. Kim, J. Immunoassay Immunochem. **27**, 31–44 (2006)
45. J.M. Burns, W.J. Cooper, J.L. Ferry, D.W. King, B.P. DiMento, K. McNeill, C.J. Miller, W.L. Miller, B.M. Peake, S.A. Rusak, Aquat. Sci. **74**, 683–734 (2012)
46. R.V. Hageman, W.H. Orme-Johnson, R. Burris, Biochem. **19**, 2333–2342 (1980)
47. N.H. Williams, J. Am. Chem. Soc. **122**, 12023–12024 (2000)